Aquaculture 592 (2024) 741223

Contents lists available at ScienceDirect

Aquaculture

journal homepage: www.elsevier.com/locate/aquaculture

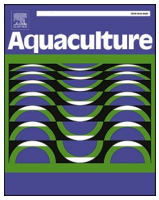

Technical paper

Echocardiography - a non-invasive alternative for assessing cardiac morphology and function in Atlantic salmon (*Salmo salar* L.)

Victoria Becker [a,b], Simona Kavaliauskiene [a,b], Erik Sandblom [c], Lucas A. Zena [c,d], Albin Gräns [d], William E. Louch [a,b], Ivar Sjaastad [a,b], Ida B. Johansen [e], Michael Frisk [a,b,*]

[a] Institute for Experimental Medical Research, University of Oslo and Oslo University Hospital Ullevål, Oslo, Norway
[b] K. G. Jebsen Center for Cardiac Research, University of Oslo, Oslo, Norway
[c] Department of Biological and Environmental Sciences, University of Gothenburg, Gothenburg, Sweden
[d] Department of Applied Animal Science and Welfare, Swedish University of Agricultural Sciences, Gothenburg, Sweden
[e] Department of Preclinical Sciences and Pathology, Faculty of Veterinary Medicine, Norwegian University of Life Sciences, Ås, Norway

ARTICLE INFO

Keywords:
Ultrasound
Repeatability
Reproducibility
Reliability
Heart physiology

ABSTRACT

Cardiac-related mortality is increasing in farmed salmon. Non-invasive tools for examining and screening for cardiac morphology and function are limited, and most common methodologies are lethal, time-consuming, and immobile. Echocardiography has previously been tested as a non-invasive, quick, and portable alternative, though its implementation is minimal. Improvements in echocardiographic techniques during the last decade have enabled more refined assessments of structure and function and hold potential for use in fish farms. Utilising a compact, transportable ultrasound system, we examined the applicability of echocardiography in Atlantic salmon (*Salmo salar* L.). Several protocols and projections were tested, and intra- and inter-variation for both operators (image acquisition) and observers (image analysis) were assessed. In addition, the accuracy of cardiac structure/function measurements was compared with standard methods. In general, high accuracy and reproducibility of cardiac dimensions and functional parameters were found within the same and between different observers analysing the same dataset (intra- and inter-observer). Measurements between recordings of the same operator (intra-operator) and between different operators (inter-operator) were less accurate and repeatable but comparable to observations in previous human and mammalian studies. Cardiac output was slightly higher when measured with echocardiography compared to transit time flow probe. Yet, a strong correlation exists between the two methods. Furthermore, morphology measured in excised hearts *ex vivo* was comparable to echocardiography measurements and strongly correlated. Thus, ultrasound presents a highly feasible, non-invasive, and swift alternative to current methods for detailed cardiac assessment of salmon hearts.

1. Introduction

The Atlantic salmon (*Salmo salar L.*) aquaculture industry experiences an alarming trend of increasing mortality rates due to various biotic and abiotic factors (Sommerset et al., 2023). One of the leading causes of rising mortality is infectious cardiac diseases such as cardiomyopathy syndrome (CMS) and heart and skeletal muscle inflammation (HSMI) (Sommerset et al., 2023). Additionally, cardiac morphological deviations (round/misshaped ventricles, enlarged/skewed bulbi) are prevalent observations in farmed salmonids and seem to be associated with risk of mortality (Sommerset et al., 2023; Engdal et al., 2024; Brijs et al., 2020). Although electrocardiography has recently shown potential for detection of myocardial ischemia in fish (Zena et al., 2024), current detection and diagnosis of cardiac-related death and deviating cardiac morphology rely heavily on *post-mortem* analyses (Engdal et al., 2024). This calls for further implementation of minimally or non-invasive tools, which can aid in early detection of cardiac-related pathology and routine cardiac health monitoring in live salmon.

Abbreviations: A, Late diastolic peak velocity; BV-valve, Bulbo-ventricular valve; CO, Cardiac output; CW, Continuous wave Doppler; E, Early diastolic peak velocity; e', Early diastolic tissue peak velocity; LAX, Longitudinal axis; MDC, Minimal detectable change; PBS, Phosphate-buffered saline; PW, Pulsed wave Doppler; RC, Repeatability Coefficient; SAX, Short axis..

* Corresponding author at: Institute for Experimental Medical Research, University of Oslo and Oslo University Hospital Ullevål, Oslo, Norway.
E-mail address: Michael.frisk@medisin.uio.no (M. Frisk).

https://doi.org/10.1016/j.aquaculture.2024.741223
Received 15 February 2024; Received in revised form 4 June 2024; Accepted 10 June 2024
Available online 11 June 2024

Echocardiography is a non-invasive, ultrasound-based imaging tool for assessing cardiac morphology and function. It is a standard technique in human and mammalian cardiac health monitoring and research (Tanaka et al., 1996; Papolos et al., 2016; Sjaastad et al., 2000). Despite minimal implementation in fish, echocardiography has previously been applied in salmonid species, including rainbow trout (*Oncorhynchus mykiss*), masu salmon (*Oncorhynchus masou masou*), and Atlantic salmon (*Salmo salar L.*) (Sande and Poppe, 1995; Usui et al., 2022; Ma et al., 2019; Cotter et al., 2008). These studies illustrated the feasibility of employing echocardiography in salmonids as a method for collecting extensive *in vivo* data sets quickly and non-invasively.

Despite these early indications of its feasibility, the method requires a thorough assessment of its ability to assess cardiac structure and function in salmon accurately. Also, its potential role in replacing methods that are either highly invasive or performed *post-mortem,* needs to be examined (Linton et al., 2004; Metcalfe and Butler, 1982; Farrell and Smith, 2017; Engdal et al., 2024). Although echocardiography has been applied in lower vertebrates since the 1990s (Chin Lai et al., 1990; Dalton et al., 1998; Sande and Poppe, 1995), no substantial efforts has been given to the precision and reliability of this method in fish. It is well established that echocardiographic measurements are prone to variability, because of bias introduced by the operator (image acquisition), the observer (image analysis), or both combined (Letnes et al., 2021; Coucelo et al., 2000). This variability, routinely considered and assessed in humans and other mammalian species, must also be carefully considered in fish. The present study established standardised protocols for performing echocardiography and data analysis in Atlantic salmon (*Salmo salar* L.). A thorough assessment of repeatability, reproducibility and reliability of the measurements showed that echocardiography is a versatile tool for collecting detailed and non-invasive information about cardiac morphology and function. We propose echocardiography as a supplementary tool for trained fish veterinarians and fish health biologists for assessment of general cardiac health in farmed Atlantic salmon. This is especially relevant when altered cardiac health is suspected.

2. Materials & methods

2.1. Ethical approval

All experiments were conducted in accordance with rules and regulations established by the Norwegian Food Safety Authority (FOTS no. 23876 and 24848).

2.2. Animals and husbandry

Twenty-six Atlantic salmon (*Salmo salar* L.) kept in sea pens at 8–15 °C (mean weight ± SD = 3856 ± 1909 g, mean fork length ± SD = 64 ± 10 cm) were used. Six individuals were used to assess intra- and inter-observer variability. Intra- and inter-operator variability were assessed in eight individuals. Twelve individuals underwent echocardiography followed by insertion of transit time flow probe. Eighteen of the included fish were additionally used to assess *ex vivo* cardiac morphology.

2.3. Anaesthesia and experimental setup

Fish were individually anaesthetised in a knockout solution containing 150 mg L^{-1} MS-222 (Tricaine methanesulfonate, Sigma-Aldrich, Missouri, USA) in seawater. When the fish became unresponsive to physical handling and operculum movement had ceased, they were transferred to a V-shaped surgical tray, draped in a wet towel, and placed ventral side up. Anaesthesia was maintained by gill irrigation in an aerated flow-through system with 75 mg L^{-1} MS-222 (Fig. 1 Ai). Temperature was adjusted to ambient water temperature (8–15 °C) and maintained by a circulating thermostatic bath (Grant Instruments, Cambridge, UK). For measuring the salmon's electrocardiogram, two platinum electrodes were inserted subcutaneously at each pectoral fin, and a reference electrode was inserted in muscle tissue between the pelvic and anal fins (Fig. 1 Ai). Electrocardiogram and heart rate were recorded continuously throughout experiments. The skin of the fish was kept hydrated by frequently pouring water over the body. Following echocardiographic examination, individuals were euthanised by a sharp blow to the head.

2.4. Standardised echocardiographic imaging and analysis

2.4.1. Echocardiography imaging

Echocardiographic image acquisition was performed using a transportable Vivid iq system from GE Vingmed Ultrasound A/S (Horten, Norway), with a 6.0/12.0 MHz phased array (paediatric cardiac) probe (12S). Morphological ventricular and atrial measurements were obtained in 2D brightness mode in two different projections: longitudinal axis (LAX), with the probe positioned parallel to the length of the fish, and short axis (SAX), with the probe positioned perpendicular to the length of the fish, across the heart (Fig. 1 Ai). The main cardiac structures observed in the LAX projection are shown and denoted in Fig. 1 Aii. To obtain standardised recordings, the caudal apex, bulbo-ventricular valve (BV-valve), and atrio-ventricular valve (AV-valve) were used as reference points in LAX (Fig. 1 Aii and Bi, ii). To visualise atrium and bulbus, the probe was moved to a more cranial position along the same axis (Fig. 1 Biii, iv). SAX recordings were acquired at the ventricle's widest point, where the atrio-ventricular valve could not be observed (Fig. 1 Bv, vi). LAX and SAX projections were used to measure global strain *i.e.* myocardial deformation through the cardiac cycle, by speckle-tracking echocardiography (Fig. 1 Bvii, viii). Anatomical motion mode was applied to ventricular LAX recordings to obtain additional information about longitudinal ventricular contractility (Fig. 1 Bix). Colour Doppler, along with continuous wave (CW) and pulse waved Doppler (PW), were recorded during the entire cardiac cycle. A representation of PW Doppler can be found in Fig. 1 Bx, xi. When recording PW for atrio-ventricular flow, the sample volume was placed at the atrio-ventricular leaflets. For ventricular-bulbus flow, the sample volume was positioned where flow velocities were deemed the highest and in the middle of the blood flow profile. Colour tissue Doppler imaging was recorded in the ventricle close to the atrio-ventricular segment.

For the largest individuals, the entire ventricle could not fit within one sector frame in LAX. Thus, the ventricle was imaged in two sectors: one acquiring the apex and dorsal part of the base and one where the ventral and dorsal base were visible throughout a cardiac cycle.

All recordings had a duration of at least three consecutive cardiac cycles, followed by a replicate recording. Duration of the complete protocol was approximately five minutes per fish.

2.4.2. Echocardiographic image analysis

All image analyses were performed using EchoPAC © analysis software (version 203).

For brightness mode recordings, ventricular dimensions were measured in both end-systole and end-diastole. These measurements included ventricular length, measured from caudal apex to base, ventricular height, measured from ventral to dorsal apex, and ventricular areas (Fig. 1 Bii). Atrial area and diameter of the bulbus and bulbo-ventricular valve were also performed in LAX (Fig. 1 Biv). Ventricular dimensions were additionally measured in SAX, including ventricle width (dorsal-dorsal apexes) and height (centre of ventral base-dorsal apex) (Fig. 1 Bvi). The nomenclature of ventricular structures is based on standardised anatomical descriptions (Engdal et al., 2024).

Anatomical motion mode was used to assess intraventricular dimensions, ejection fraction and fractional shortening in LAX view. During image analysis, the anatomical motion mode cursor was placed through the caudal apex and dorsal bulbus attachment of the ventricular base (caudal apex to base) (Fig. 1 Bix).

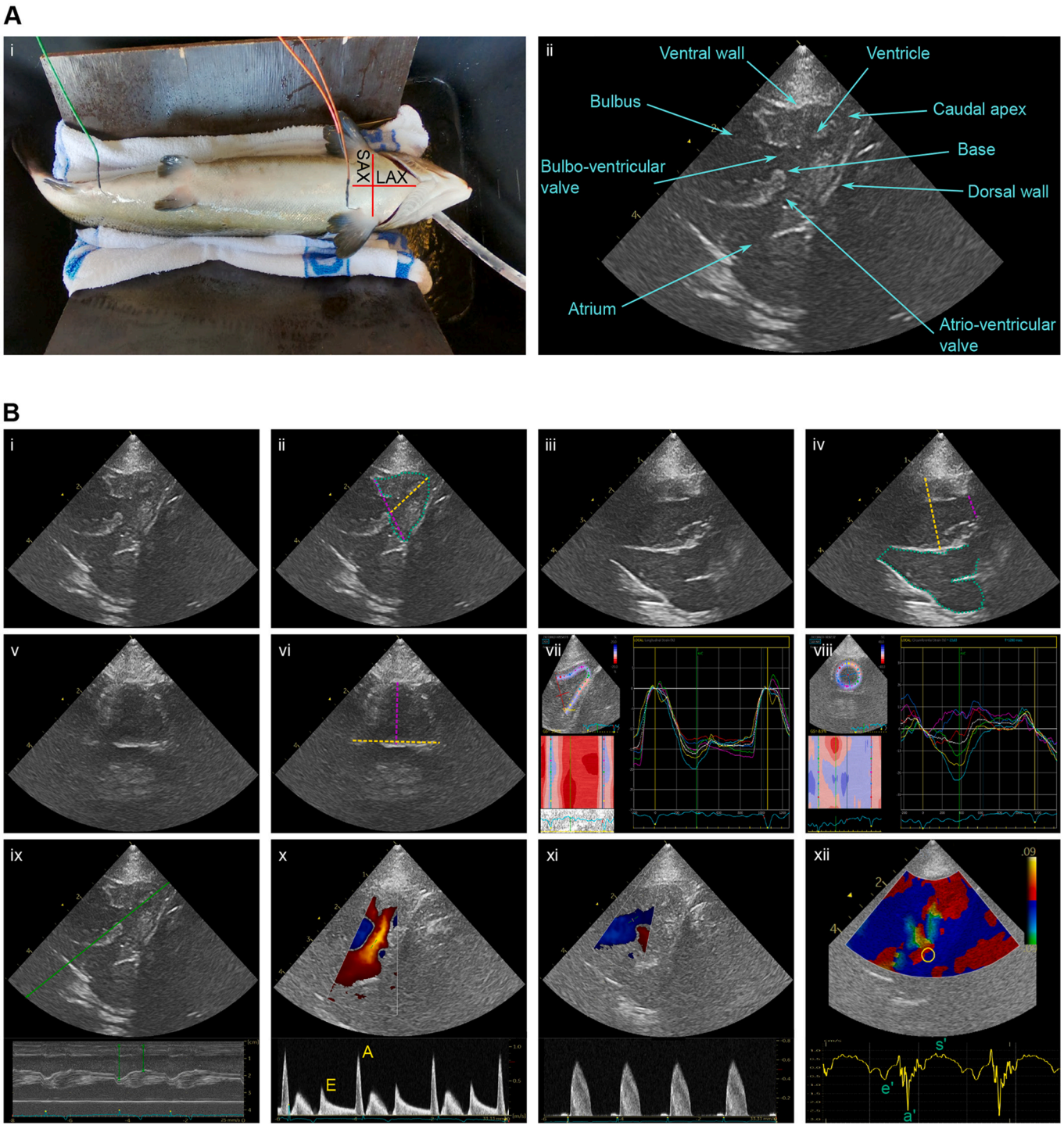

Fig. 1. Experimental setup and echocardiographic imaging and analysis.
Ai Experimental setup showing placement of ECG electrodes and echocardiographic probe orientation (longitudinal axis (LAX) and short axis (SAX)). **Aii** and **Bi** Representative LAX echocardiography with key cardiac structures indicated. **Bii** Ventricular dimensions illustrated, including ventricle length (caudal apex to base) (yellow), height (ventral-dorsal height) (purple), and ventricular area (green). **Biii** Typical 2D LAX recording of bulbus and atrium. **Biv** Depiction the bulbo-ventricular valve (BV-valve) diameter (purple), bulbus diameter (yellow) and atrial area measurements (green). **Bv** Cardiac phased array probe (2D SAX). **Bvi** Ventricular dimensions in SAX (ventricular width (dorso-dorsal width, yellow) and height (ventro-dorsal height, purple). **Bvii** Longitudinal speckle tracking trace measured in LAX. **Bviii** Circumferential speckle tracking trace (SAX). **Bix** Anatomical motion-mode (am-mode) from caudal apex to base. **Bx** Diastolic haemodynamics (atrioventricular) showing both early (E) and late (A) blood flow velocities recorded by pulsed wave (PW) Doppler. **Bxi** Systolic haemodynamics (ventricular outflow tract) recorded by PW Doppler. **Bxii** Representative colour tissue Doppler imaging and velocity trace exhibiting e': early diastolic tissue velocity, a': late diastolic tissue velocity, and s': peak systolic tissue velocity. (For interpretation of the references to colour in this figure legend, the reader is referred to the web version of this article.)

Haemodynamics were analysed using colour Doppler, with an initial assessment of the direction of blood flow employed for angle correction in further analyses (Fig. 1 Bx, xi). Next, diastolic (atrio-ventricular valve) and systolic (bulbo-ventricular valve) blood flow velocities were recorded with both CW and PW Doppler (Fig. 1 Bx, xi). Peak and mean blood flow velocity measurements were obtained together with the velocity time integral and envelope time. Stroke volume (SV) and cardiac output (CO) were calculated as proposed by Ma and colleagues for salmonids (Ma et al., 2019). This equation corrects for the distinct haemodynamic pattern observed in fish compared to mammals by using the approximate velocity time integral median instead of the maximum. Diastolic function was assessed based on measurements of early diastolic peak velocity (E) and late diastolic peak velocity (A) (Fig. 1 Bx).

Colour tissue Doppler imaging analyses were performed at the dorsal apex of the ventricle near the atrioventricular canal on the ventricular dorsal wall (the area close to the atrio-ventricular segment). A circular sample area with a 4 mm diameter was used. Colour tissue Doppler imaging was employed to determine early diastolic tissue velocity (e') (Fig. 1 Bxii). Full analysis of the echocardiographic recordings took between 10 and 20 min per fish.

2.5. Intra- and inter-variability

Variability within echocardiographic measurements appears during image analysis (observer) and image acquisition (operator). This variability can occur within the same (intra) or between different (inter) observers and operators. Therefore, intra- and inter-observer variability were assessed. To calculate intra-observer variability, each echocardiographic parameter was measured twice by the same person, with a period of at least 24 h between measurements to minimise memory bias. For assessment of inter-observer variability, parameters were measured once by two different observers, who were blinded to each other's measurements.

For intra- and inter-operator variability, one operator performed two complete consecutive recordings (intra-operator), with a minimum of five minutes between repeated measurements. Afterwards, a second operator conducted one full recording, which was compared with recordings acquired by the first operator (inter-operator).

2.6. Ex vivo morphological measurements

To validate cardiac dimensions obtained by echocardiography, cardiac structures were determined *ex vivo*. Following *in vivo* examination, hearts were carefully excised and rinsed in phosphate-buffered saline (PBS) (Dulbecco's Phosphate Buffered Saline, EuroClone, Milan, Italy). Once cleared of blood, hearts were transferred to PBS containing 50 mM KCl to induce cardiac arrest in diastole. Samples were fixed in buffered 4% formaldehyde solution (HistoLab, Hønefoss, Norway) for 1–2 days before being transferred to PBS containing 0.02% sodium azide (NaN_3) and stored at 4–8 °C. *Ex vivo* heart morphology was assessed as described by Engdal et al. (2024). In brief, photographs were captured with a camera (Canon E05 (DS126151)), mounted on a styrofoam box with fixed light conditions. Ventricular length, height, and bulbus width were measured using ImageJ (Schindelin et al., 2012).

2.7. Cardiac output from transit time ultrasonic flow probe

To verify echocardiography-based CO calculations, a subset of 12 individuals underwent surgical insertion of a transit time blood flow probe (2.5 PSL, Transonic Systems, NY, USA) around the ventral aorta (McArley et al., 2021) after completion of all echocardiographic recordings. In brief, a small incision was made at the ventral base of the opercular cavity, the ventral aorta was dissected free, and the probe was placed around the vessel. CO and heart rate were then recorded in the anaesthetised fish using a PowerLab system with LabChart pro data acquisition software (version 7.3.28.1.21, ADInstruments, Castle Hill, Australia). All flow probes were calibrated at test temperature according to the manufacturer's instructions (see Morgenroth et al. (2021).

2.8. Data and statistical analyses

All echocardiographic measurements are presented as the mean of three consecutive cardiac cycles. Cardiac output and heart rate data from transit time blood flow measurements are reported as means over a one-minute period when flow signals were stable.

All statistical analyses and calculations for assessing variability components were performed in Graphpad Prism © (version 9.3.1, La Jolla, CA, United States) and Microsoft Excel (2016, Redmond, WA, United States).

2.8.1. Repeatability

Repeatability describes the variation of repeated measurements and analyses on the same subject under identical conditions and is dependent only on the measurement and analysis process itself and not the variation in the subject or conditions. Thus, repeatability was assessed for image analysis (intra-observer) and image acquisition (intra-operator). Repeatability was assessed using the repeatability coefficient (RC), calculated as within-subject standard deviation $\times$ 1.96 $\times$ $\sqrt{2}$ (Letnes et al., 2021; Bartlett and Frost, 2008). Thus, low RC values indicate good repeatability. RCs are presented as mean absolute values for the whole population with 95% confidence intervals (CIs). Additionally, RC is presented as a percentage of the mean value for the population of each variability component.

2.8.2. Reproducibility

Reproducibility is defined as the variation in a measurement made on a subject under changing conditions. In real-life situations, it is impossible to exclude changes in measurement method, observer (vision and perception), location, and other environmental factors, and all of them will affect the reproducibility of a measurement. To estimate reproducibility of morphological and functional parameters obtained by echocardiography in Atlantic salmon, agreement and bias were assessed by Bland Altman analyses (Bunting et al., 2019; Bartlett and Frost, 2008; Bland and Altman, 1996). Bias is the mean difference between measurements, and limits of agreement indicate the interval within which 95% of the difference will fall. In addition, Pearson's correlation coefficient was used to describe the association between measurements for all variability components (Bunting et al., 2019).

2.8.3. Reliability

The reliability of a method depends on both the magnitude of measurement error and the heterogeneity of a population. Thus, reliability indicates to what degree a given method can differentiate between subjects or groups. To assess reliability, minimal detectable change (MDC) was determined for each individual fish, calculated as within-subject standard error of the mean $\times$ 1.96 $\times$ $\sqrt{2}$ (Bunting et al., 2019). Mean MDC of the entire population was then calculated as a percentage, along with the 95% CI. Thus, MDC represents the minimal change (in percentage) required to ensure that a detected difference reflects biological change and not merely measurement error (Bunting et al., 2019).

2.8.4. Validation of echocardiographic measurements

We performed Pearson's correlation and Bland Altman analyses to determine agreement and association between results acquired by echocardiography and established methods (*ex vivo* cardiac morphology and transit time flow probe measurements). Statistical analysis of bias in *ex vivo* and *in vivo* measurements was performed with paired *t*-tests (Bartlett and Frost, 2008). A p-value <0.05 was considered statistically significant.

3. Results & discussion

The ability of echocardiography to provide reliable and repeatable quantification of cardiac morphology and function was evaluated to assess its potential for observing and monitoring cardiac health in farmed salmon. To this end, we developed standardised imaging and analysis protocols and assessed intra- and inter-variability to confirm the usefulness and robustness of the method.

3.1. Standardised echocardiographic imaging and analysis

Establishing the best imaging projections and modalities encompasses a thorough evaluation of image quality, signal strength, and clear reference points for standardisation. During preliminary testing, several projections (SAX, LAX, bi-plane) and imaging modalities (brightness mode, motion mode, speckle tracking, tissue velocity imaging, colour tissue Doppler imaging, flow Doppler) were assessed. The most feasible and promising projections and image modalities were chosen based on initial screening. Together, they yield sufficient information for performing a thorough assessment of cardiac anatomy and function. These projections and image modalities are presented in Figure 1.

Superior image quality was achieved in LAX, but cardiac dimensions could be determined in both LAX and SAX (Fig. 1 Bi-vi). We observed that ventricular dimensions were more easily assessed in brightness mode than anatomical motion mode (Fig. 1 Bii, ix). Likely, this is due to the presence of spongious myocardium, blurring the separation between lumen and myocardium and thereby hindering clear identification of ventricular walls in anatomical motion mode. By speckle-tracking echocardiography, global strain was feasible in both SAX and LAX (Fig. 1 Bvii, viii). However, assessment of global longitudinal strain was challenging in large fish where the entire ventricle could not be captured in one frame. This limitation hindered automatic recognition of tissue borders by Echopac ©, thereby rendering strain analyses difficult.

Haemodynamics were first visualised *via* colour Doppler and then measured using both CW and PW Doppler to assess diastolic (Fig. 1 Bx) and systolic function (Fig. 1 Bxi). Due to the range gating of the PW Doppler, we found that this modality was best suited for performing blood velocity measurements at defined locations, such as the atrio-ventricular and bulbo-ventricular valve. We also found that, compared to SAX, LAX allows a broader range of angle adjustments and provided higher blood velocity recordings. Thus, LAX is recommended over SAX for blood velocity assessment. Further, measuring tissue velocities by colour tissue Doppler imaging (Fig. 1 Bxii) was easier to standardise than directly recording the tissue velocity profile during image acquisition with PW Tissue Doppler.

In the current study, we included fish only above 1200 g, but a similar echocardiographic probe has previously been applied on zebrafish (Wang et al., 2017). Despite being possible to utilise echocardiography in smaller fish, it requires a stationary, more powerful system that is less versatile. Such a setup is less suitable for the sea phase of aquaculture, where space is often limited, and several locations usually are of interest.

3.2. Repeatability, reproducibility, and reliability

Variability in echocardiographic image acquisition and analysis critically affects the acquired data's repeatability, reproducibility, and reliability. Thus, intra-observer, inter-observer, intra-operator, and inter-operator variability were evaluated for all measured parameters. Main results are summarised in Table 1 (See Supplementary Table A.1 for the complete dataset).

3.2.1. Repeatability

Except for diastolic atrial area, dimensional intra-observer repeatability of cardiac structures was high with RCs below 10% of reference values (Table 1). Notably, this level of intra-observer repeatability is equal to or lower than that reported in most human and mammalian studies (Letnes et al., 2021; Gentile-Solomon and Abbott, 2016; Berthoud and Schwarzwald, 2021). For functional parameters, intra-observer repeatability was somewhat lower (RCs ranging from 6.88 to 30.17%, Table 1). Still, these values are within the range reported for human patients (Letnes et al., 2021). Global circumferential strain, e' and E/e' measurements, displayed the highest RCs (Table 1). Likely, this reflects that these analyses depend on manual selection of specific tissue. Additionally, the presence of spongious myocardium can affect decisions on what is included in the analysis (Coucelo et al., 2000).

Repeatability was also examined for the same operator on two consecutive recordings (intra-operator repeatability). RCs were generally higher compared to the results obtained for intra-observer analyses (Table 1). This was expected since image acquisition reportedly accounts for a more significant portion of variability than image reading within repeated measurements (Letnes et al., 2021). In comparison with other parameters, lower intra-operator repeatability was evident for measurements of atrial area (Table 1), which likely reflects a lack of robust reference points for atrial recordings. Fish size and amount of adipose tissue may also play a role since bigger fish (the requirement for deeper probe range) and excessive adipose tissue dampen the ultrasound signal (Ellenberger et al., 2022). Thus, the use of different cardiac probes or altered probe settings optimised for atrial imaging could perhaps improve the outcome. Intra-operator repeatability was also significantly lower for measures of diastolic function (E/A, e', E/e', Table 1). This was partly due to operator variability, although physiological alterations occurring throughout the echocardiographic protocol are also a well-known contributor (Letnes et al., 2021; Mirea et al., 2019). For example, stress prior to anaesthesia elevates catecholamine levels (Demers and Bayne, 1997), which in turn increases central venous blood pressure (Skals et al., 2006; Sandblom et al., 2009). Since early diastolic blood flow velocity (E) is driven by the pressure gradient between the atrium and ventricle, altered central venous blood pressure will acutely affect E values. Catecholamines, particularly adrenaline, are quickly cleared from the bloodstream (Randall and Ferry, 1992; Nekvasil and Olson, 1986). Consequently, a stressed individual will exhibit higher E velocities at the onset of examination compared to a few minutes later. Thus, the relatively high variation observed in E in the current study likely reflects these time-dependent changes. Hence, it is important to be conscious of stress levels and take precautions to minimise E variation. Despite the variability observed in E, the peak velocities in the current study are similar to those reported for other salmonid species (Usui et al., 2022).

3.2.2. Reproducibility

Reproducibility was assessed by quantifying association (Pearson correlation) and bias (Bland Altman analysis) (Table 1). Strong associations and low bias values indicated that high reproducibility was generally observed for intra-observer and intra-operator comparisons. The somewhat lower reproducibility observed for intra-operator diastolic functional parameters is likely attributed to time- and stress-dependent physiological alterations (discussed in section 3.2.1.) rather than methodological limitations.

As expected, reproducibility was lower for inter-observer and -operator, compared to values obtained for the same observer and operator. This phenomenon is a common finding, well-documented in mammalian and zebrafish studies (Wang et al., 2017; Hsue and Visser, 2020) and emphasises the benefit of using the same observer and operator during data collection. An additional well-known contributing factor of inter-operator variability is the experience and training of operators (Coucelo et al., 2000; DeCara et al., 2003; Labbé et al., 2016; Vignon et al., 2011). This should also be considered when designing a study or screening populations during routine health controls in aquaculture.

Table 1
Repeatability, reproducibility, and reliability of key cardiac dimensions and functional parameters in Atlantic salmon.

	Bias & agreement			Association					
	Bias (s.d.)	Limits of agreement		r	p	Mean RC (% of reference value)	95% CI	Mean MDC	95% CI
		Lower	Upper						
Ventricular length (s) (mm) (LAX)									
Intra-observer variability	0.22 (0.49)	−0.74	1.19	0.89	0.02	1.40 (8.15)	0.19 to 2.61	5.76	0.78 to 10.75
Inter-observer variability	0.80 (1.56)	−2.26	3.85	0.67	0.14			9.92	5.88 to 13.95
Intra-operator variability	−0.81 (1.91)	−4.56	2.94	0.78	0.02	3.12 (14.86)	1.45 to 4.79	10.51	4.88 to 16.13
Inter-operator variability	−0.03 (1.26)	−2.50	2.44	0.90	0.00			7.06	4.62 to 9.49
Ventricular length (d) (mm) (LAX)									
Intra-observer variability	0.13 (0.16)	−0.18	0.44	0.99	0.00	0.68 (3.26)	0.37 to 0.99	2.31	1.24 to 3.37
Inter-observer variability	0.71 (1.00)	−1.26	2.67	0.89	0.02			6.81	5.42 to 8.20
Intra-operator variability	−0.64 (1.62)	−3.81	2.53	0.90	0.00	2.08 (8.23)	0.26 to 3.90	5.82	0.74 to 10.90
Inter-operator variability	−1.30 (1.76)	−4.74	2.14	0.88	0.00			9.56	4.88 to 14.25
Ventricular height (s) (mm) (LAX)									
Intra-observer variability	0.12 (0.67)	−1.20	1.43	0.93	0.01	1.06 (5.18)	0.53 to 1.60	3.67	1.83 to 5.50
Inter-observer variability	3.37 (1.75)	−0.07	6.80	0.51	0.30			19.54	15.38 to 23.70
Intra-operator variability	−0.48 (1.48)	−3.39	2.42	0.82	0.01	2.37 (11.04)	1.16 to 3.58	7.81	3.82 to 11.79
Inter-operator variability	−0.22 (1.73)	−3.61	3.17	0.80	0.02			8.27	3.45 to 13.09
Ventricular height (d) (mm) (LAX)									
Intra-observer variability	−0.46 (1.10)	−2.63	1.70	0.96	0.00	1.85 (8.04)	0.84 to 2.85	5.68	2.59 to 8.78
Inter-observer variability	−1.95 (0.77)	−3.45	−0.45	0.95	0.00			12.86	10.70 to 15.02
Intra-operator variability	−1.01 (0.80)	−2.58	0.56	0.96	0.00	2.22 (9.45)	1.44 to 3.01	6.68	4.33 to 9.04
Inter-operator variability	−0.09 (1.89)	−3.79	3.61	0.79	0.02			8.63	4.32 to 12.94
Atrial area (s) (mm^2) (LAX)									
Intra-observer variability	2.32 (2.24)	−2.07	6.70	1.00	0.00	10.19 (6.87)	4.45 to 15.92	4.86	2.12 to 7.59
Inter-observer variability	19.86 (23.83)	−26.84	66.56	0.96	0.00			16.37	13.40 to 19.34
Intra-operator variability	−15. 95 (27.58)	−70.01	38.12	0.92	0.00	58.55 (35.03)	40.04 to 77.05	24.77	16.40 to 33.14
Inter-operator variability	−12.80 (21.54)	−55.03	29.42	0.98	0.00			18.13	9.38 to 26.87
Atrial area (d) (mm^2) (LAX)									
Intra-observer variability	−1.19 (3.96)	−8.96	6.58	0.99	0.00	12.76 (10.57)	5.95 to 19.57	7.74	3.48 to 11.46
Inter-observer variability	20.43 (17.71)	−14.29	55.15	0.99	0.00			20.19	17.30 to 23.08
Intra-operator variability	−0.07 (32.49)	−63.74	63.60	0.88	0.00	57.39 (43.13)	36.76 to 78.03	30.50	18.78 to 42.22
Inter-operator variability	−8.84 (24.23)	−56.33	38.64	0.95	0.00			22.49	10.41 to 34.56
BV- valve diameter (mm) (LAX)									
Intra-observer variability	0.02 (0.11)	−0.18	0.24	0.98	0.00	0.16 (4.12)	0.06 to 0.26	2.92	1.13 to 4.70
Inter-observer variability	0.21 (0.46)	−0.69	1.12	0.70	0.12			12.58	2.55 to 22.61
Intra-operator variability	0.05 (0.15)	−0.24	0.34	0.98	0.00	0.24 (5.50)	0.13 to 0.35	3.89	2.03 to 5.75
Inter-operator variability	−0.90 (1.65)	−4.14	2.33	0.92	0.00			10.57	4.18 to 16.95
Bulbus diameter (s) (mm) (LAX)									
Intra-observer variability	−0.10 (0.26)	−0.60	0.41	0.96	0.00	0.75 (4.75)	0.18 to 1.32	3.36	0.80 to 5.92
Inter-observer variability	−0.18 (0.61)	−1.37	1.06	0.98	0.00			4.32	2.73 to 5.90
Intra-operator variability	0.16 (0.37)	−0.57	0.89	0.99	0.00	0.64 (3.68)	0.34 to 0.93	2.61	1.38 to 3.83
Inter-operator variability	−0.50 (1.33)	−3.11	2.11	0.85	0.01			7.52	1.80 to 13.24
Bulbus diameter (d) (mm) (LAX)									
Intra-observer variability	−0.11 (0.25)	−0.59	0.38	0.94	0.01	0.68 (4.91)	0.05 to 1.30	3.47	0.28 to 6.66
Inter-observer variability	−0.45 (0.77)	−1.96	1.06	0.94	0.01			7.41	4.37 to 10.09
Intra-operator variability	1.08 (0.72)	−0.33	2.48	0.96	0.00	2.11 (13.83)	1.14 to 3.08	9.78	5.27 to 14.29
Inter-operator variability	−1.20 (1.32)	−3.79	1.40	0.81	0.01			12.79	6.11 to 19.47
Stroke volume (mL)									
Intra-observer variability	0.17 (0.41)	−0.63	0.97	0.99	0.00	0.33 (7.00)	−0.31 to 0.97	4.95	−4.75 to 14.65
Inter-observer variability	0.33 (1.03)	1.69	2.35	0.87	0.03			18.48	0.37 to 36.59
Intra-operator variability	0.13 (1.55)	−2.92	3.17	0.94	0.00	2.21 (28.00)	0.86 to 3.55	20.18	7.84 to 32.40
Inter-operator variability	−3.63 (3.07)	−9.64	2.39	0.90	0.01			47.77	24.31 to 71.23
Cardiac output (mL min^{-1})									
Intra-observer variability	5.29 (11.50)	−17.25	27.83	0.98	0.00	19.44 (10.64)	8.61 to 30.27	7.53	3.33 to 11.72
Inter-observer variability	34.30 (55.31)	−74.11	142.72	0.75	0.08			30.30	8.78 to 51.81
Intra-operator variability	−13.32 (28.88)	−69.92	43.28	0.95	0.00	45.10 (22.99)	16.89 to 73.32	16.26	6.09 to 26.43
Inter-operator variability	−43.48 (75.56)	−191.16	104.61	0.69	0.08			43.63	24.32 to 60.93
Fractional shortening (%)									
Intra-observer variability	0.17 (3.25)	−6.20	6.54	0.96	0.00	4.25 (23.81)	0.75 to 7.74	16.84	2.98 to 30.70
Inter-observer variability	9.17 (5.81)	−2.22	20.56	0.70	0.12			47.05	23.19 to 70.92
Intra-operator variability	4.00 (7.65)	−11.00	19.00	0.48	0.27	4.48 (26.35)	2.01 to 6.95	18.63	8.34 to 28.93
Inter-operator variability	−4.75 (6.69)	−17.87	8.37	−0.14	0.74			27.95	4.86 to 51.04
GCS (%)									
Intra-observer variability	−0.43 (1.87)	−4.10	3.23	0.95	0.00	2.55 (23.06)	0.51 to 4.59	19.57	6.48 to 32.29
Inter-observer variability	1.00 (6.08)	−10.92	12.92	0.47	0.00			37.95	−0.76 to 76.67
Intra-operator variability	−2.41 (5.49)	−13.17	8.34	−0.22	0.64	9.66 (75.12)	5.41 to 13.91	53.12	21.92 to 56.41

(*continued on next page*)

Table 1 (*continued*)

	Bias & agreement			Association					
	Bias (s.d.)	Limits of agreement		r	p	Mean RC (% of reference value)	95% CI	Mean MDC	95% CI
		Lower	Upper						
Inter-operator variability	1.81 (4.74)	−7.48	11.11	0.43	0.33			39.26	12.94 to 65.58
E/A (PW)									
Intra-observer variability	−0.01 (0.01)	−0.03	0.02	0.99	0.00	0.02 (6.88)	0.01 to 0.03	4.86	1.38 to 8.34
Inter-observer variability	0.00 (0.04)	−0.08	0.08	0.97	0.00			13.86	2.67 to 25.04
Intra-operator variability	−0.06 (0.09)	−0.23	0.10	0.78	0.02	0.15 (98.00)	0.06 to 0.25	69.30	26.75 to 111.85
Inter-operator variability	−0.06 (0.09)	−0.25	0.12	0.02	0.97			82.50	46.06 to 118.93
e′ (mm s^{-1})									
Intra-observer variability	−0.23 (1.43)	−3.03	2.58	0.99	0.00	1.85 (27.23)	0.23 to 3.47	19.26	2.36 to 36.16
Inter-observer variability	−1.70 (5.74)	−12.95	9.55	0.09	0.85			85.85	−33.63 to 205.34
Intra-operator variability	−0.64 (7.37)	−15.09	13.81	−0.34	0.45	9.55 (158.00)	0.81 to 18.29	111.73	9.44 to 214.01
Inter-operator variability	0.19 (5.95)	−11.48	11.85	−0.07	0.89			63.84	6.98 to 120.69
E/e′ (PW)									
Intra-observer variability	−3.93 (0.30)	−22.16	14.29	0.99	0.00	12.23 (30.17)	0.36 to 24.07	21.34	0.63 to 42.04
Inter-observer variability	17.97 (39.55)	−59.55	95.49	0.86	0.01		−1.11 to 107.44	61.61	−1.28 to 124.51
Intra-operator variability	11.54 (99.59)	−183.65	206.73	−0.13	0.78	108.49 (202.02)	−22.77 to 239.76	142.85	−29.98 to 315.68
Inter-operator variability	−39.32 (86.77)	−209.24	130.76	−0.45	0.36			133.00	−71.65 to 337.64

Repeatability was assessed by calculation of repeatability coefficients (RCs) presented as a mean absolute value and as a percentage of reference value (in brackets), along with 95 % confidence intervals of absolute values (CI). Bias and limits of agreement (absolute values derived from Bland Altman analysis) and association between measurements (Pearson correlation coefficient (r)) were used to evaluate reproducibility. Reliability of all measurements was assessed by calculating minimal detectable change (MDC) presented as a population mean in percentage along with 95% CI. BV-valve: bulbo-ventricular valve, LAX: Longitudinal axis, PW: pulsed wave Doppler, (s): end-systole, (d): end-diastole, E/A: early diastolic velocity / late diastolic velocity, e': early diastolic tissue velocity, GCS: global circumferential strain. $n_{Intra\text{-}observer} = 6$, $n_{Inter\text{-}observer} = 6$, $n_{Intra\text{-}operator} = 8$, $n_{Inter\text{-}operator} = 8$.

3.2.3. Reliability

Reliability was assessed by calculating the minimal detectable change (MDC) for all measurements. High intra-observer reliability was observed for all parameters (Table 1). In line with previous findings, reliability was somewhat lower between two observers (Table 1) (Decloedt et al., 2017; Dukes-McEwan et al., 2002). These studies also highlighted that acquiring reliable functional measurements is more challenging than morphological data. In agreement with this, we observed that larger differences are needed to detect true functional alterations. In particular, we observed that operator reliability was challenging when measuring diastolic function (Table 1) due to the physiological changes that can occur over time (discussed in section 3.2.1.) and the different experience levels of the operators. High reliability is especially critical when performing longitudinal studies or following populations over time, and our results indicate that the same operator and observer should perform recordings and analyses to obtain the most reliable measurements. Alternatively, precautions should be taken to ensure appropriate staff training and performance testing to confirm that reliable data is obtained when multiple operators and/or observers are involved.

3.3. Validation of echocardiographic measurements

3.3.1. Cardiac output

While it is critical that repeatability, reproducibility and reliability analyses are performed when implementing new methods, it is equally important to verify that the measurements obtained are indicative of actual physiological status. Currently, few tools for measuring *in vivo* cardiac function are available for fish, and the present standard method for measuring CO is transit time flow probe (Farrell and Smith, 2017). To evaluate the applicability and accuracy of echocardiography for measuring CO in salmon, 12 fish underwent surgical implantation of flow probe following echocardiography (Fig. 2 A). A positive correlation ($r = 0.78$, $p < 0.05$) was evident between CO obtained from echocardiography and the flow probe (Fig. 2 Aiv). Not surprisingly, CO derived from echocardiography was slightly higher (×1.48) than probe measurements (Fig. 2 Av), which is also a common phenomenon in mammalian research (Tournoux et al., 2011). This discrepancy is likely caused by a suboptimal angle of the echocardiography probe during recordings. This necessitates angle correction in post-analyses, a factor known to introduce uncertainty in velocity measurements (Reef, 1991; Kebed et al., 2020) and, therefore, in CO calculations. The maximal angle correction and whether angle correction should be applied at all is subject to debate (Quiñones et al., 2002). A common cut-off value is 60° (Jiang et al., 2011), though one study found that measurement errors can be observed at lower angles (Winkler and Wu, 1995). In this study, angle corrections between 45 and 60° were used, and the observed overestimation of CO suggests that angle correction should be more limited when conducting echocardiography on fish. Potential measures that could be performed to alleviate this issue include using echocardiographic gel and tilting the probe (both physically and internally). These modifications can help position the ultrasound beam more parallel to the blood flow axis (Quiñones et al., 2002). Exposure to and time period of anaesthesia is known to affect cardiovascular function, including decreased heart rate (Randall and Smith, 1967) and contractility (Hill et al., 2002; Ryan et al., 1993). In the present study, transit time flow probe measurements were performed after echocardiography. Although we did not observe any differences in heart rate between these two measurements (mean HR ± SD with echocardiography = 47 ± 10 *vs* flow probe 42 ± 6, $p = 0.09$), it cannot be excluded that the discrepancies between the two CO measurements were affected by reduced cardiac contractility. In addition, using CO calculations directly derived from analyses in EchoPAC© yields significantly higher (×2.97) CO values compared to flow probe measurements (Fig. A.1ii), which is most likely attributed to differences in velocity time integral tracing between fish and mammals. Yet, they correlate significantly with values measured by the flow probe (Fig. A.1i). Despite the described challenges with angle correction and anaesthesia exposure, we believe that echocardiography can be successfully applied to evaluate CO in salmon and allow for quick screening of groups or monitoring changes over time. Thus, although prone to overestimation, echocardiography can be a fast, versatile and non-invasive method for assessment of CO in the salmon aquaculture industry.

3.3.2. Morphology

To examine the accuracy of morphological measurements obtained

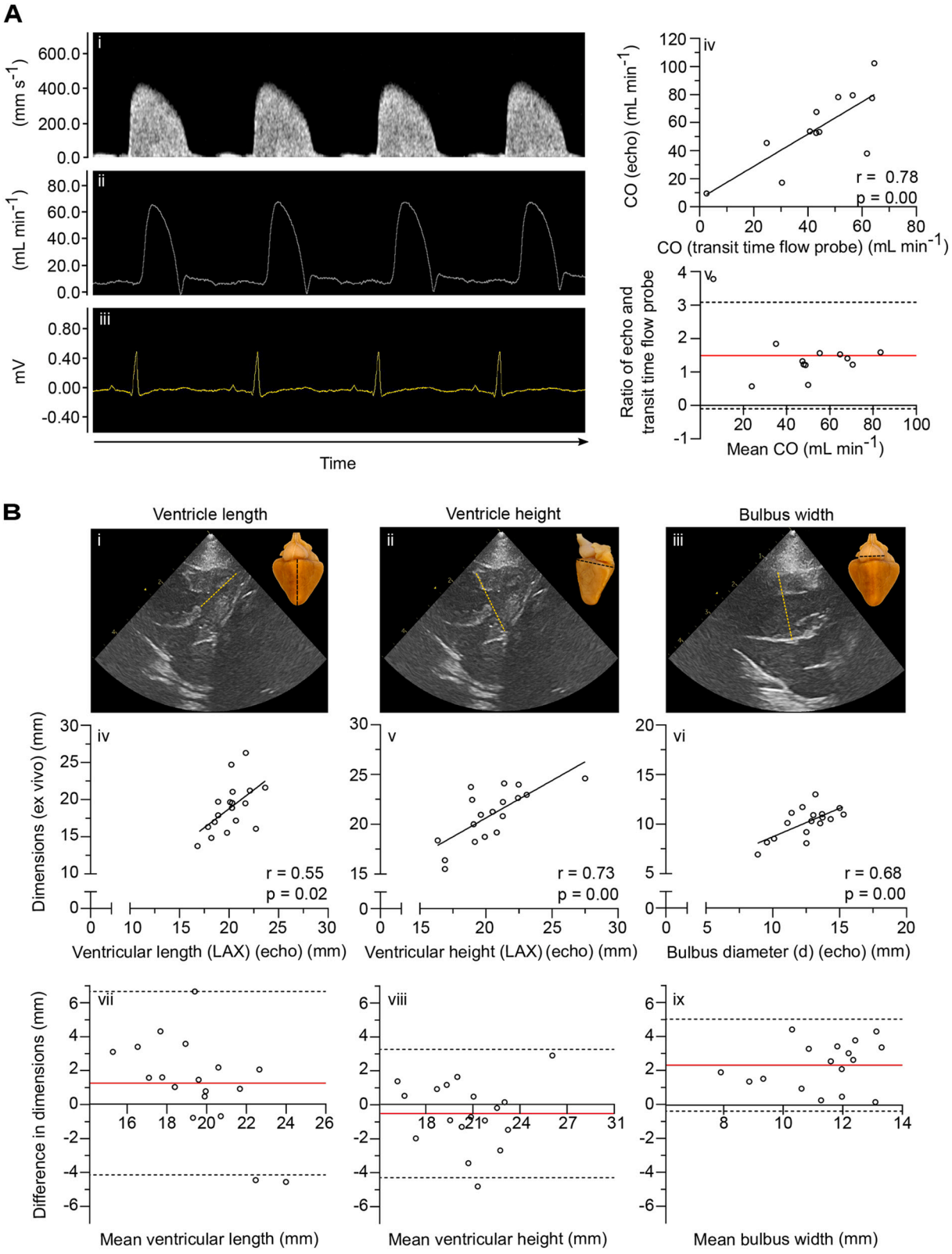

Fig. 2. Validation of echocardiographic measurements.
A Measurements of cardiac output based on flow measurements from (i) bulbo-ventricular valve (BV-valve) velocity traces (mm s^{-1}) captured through echocardiography, and (ii) flow measurements (mL min^{-1}) obtained through transit time flow probe placed on ventral aorta, along with (iii) electrocardiographic recordings (representative recordings). (iv) Correlation plot of cardiac output (CO) obtained from transit time flow probe and calculation of CO (from Ma et al., (2019)) based echocardiographic recordings, and (v) Bland Altman plot showing the ratio of differences between the two methods of estimating CO; $n = 12$. **B** Agreement and correlation of morphological dimensions measured (i-iii) *ex vivo* and *in vivo* by echocardiography in diastole and presented by (iv-vi) correlation plots and (vii-ix) associated Bland Altman plots showing differences in absolute values; $n = 18$.

by echocardiography, hearts were evaluated *ex vivo* as previously described (Engdal et al., 2024). Fig. 2 B(i-iii) depicts echocardiographic and corresponding *ex vivo* measurements. Cardiac dimensions correlated strongly (Fig. 2 Biv-vi), and though a slight bias was present, no significant differences ($p > 0.05$) were observed for ventricular dimensions (Fig. 2 Bvii, viii). In contrast, bias was observed for bulbus measures, where echocardiographic measurements indicated larger bulbus *in vivo* (Fig. 2 Bix). A likely explanation for this is that the reservoir-like properties of the bulbus hinder complete emptying between cardiac cycles *in vivo* (Braun et al., 2003). Thus, the bulbus is inflated (more or less) at any time during the cardiac cycle *in vivo*, while it is not *ex vivo*. Hence, this discrepancy reflects actual differences *in vivo* compared to *ex vivo* rather than resulting from measurement error. Taken together, our data indicate that echocardiography can not only replace *ex-vivo* post-mortem assessment of cardiac morphology but also facilitates non-invasive early detection of morphological or cardio-pathological changes in live fish.

3.4. Implementation of echocardiography in aquaculture

The protocol employed for echocardiography in this article were designed to achieve the most detailed information possible and to establish what read-outs are most critical for interpretation of cardiac health status. However, recording and analysis time, can be significantly shortened by reducing the number of captures, and highly informative data can be obtained by recording only three projections: 2D LAX and PW Doppler velocities in the AV and BV valves. These recordings enable measurements of basic morphology, systolic and diastolic hemodynamics and contractility.

Currently, data analysis takes about 15 min and must be performed manually. Machine learning and artificial intelligence are, however, an obvious possibility to automate these analyses in the future. Thus, echocardiography is already a quick *in vivo* alternative for studying cardiac shape and function for research purposes and possesses great potential for future large-scale use in aquaculture.

Anaesthesia is a prerequisite for performing echocardiography and more research is required to address how findings at rest manifest in free/maximally swimming individuals. While one approach could be to inject a combination of isoprenaline and atropine to induce maximum heart rate during echocardiographic recordings (Casselman et al., 2012), it should be noted that others have reported that such an intervention does not accurately reflect the physiology of free-swimming fish either (Sandrelli and Gamperl, 2023). Despite these difficulties in translation to the natural setting, we maintain that echocardiography can be useful for comparing cardiac health, both within and between fish populations, when anaesthesia conditions are carefully controlled.

4. Conclusion

Our results show that echocardiography is highly feasible in Atlantic salmon, allowing assessment of both structural and functional parameters. Our results demonstrate a new possibility for fast, improved surveillance and follow-up of aquaculture populations where cardiac issues are suspected. With certain methodological precautions, we show that echocardiographic measurements are repeatable, reproducible and reliable and yield results comparable to conventional, invasive methods for investigating cardiac (patho)physiology in fish. Thus, echocardiography is a non-invasive and versatile technique for cardiac evaluation in Atlantic salmon. Additionally, given the mobility of modern systems, echocardiography offers cardiac assessment at any location.

Supplementary data to this article can be found online at https://doi.org/10.1016/j.aquaculture.2024.741223.

CRediT authorship contribution statement

Victoria Becker: Writing – original draft, Visualization, Methodology, Investigation, Formal analysis, Data curation. **Simona Kavaliauskiene:** Writing – review & editing, Supervision, Investigation, Formal analysis, Data curation. **Erik Sandblom:** Writing – review & editing, Methodology, Investigation. **Lucas A. Zena:** Writing – review & editing, Methodology, Investigation. **Albin Gräns:** Writing – review & editing, Methodology, Investigation. **William E. Louch:** Writing – review & editing, Supervision. **Ivar Sjaastad:** Writing – review & editing, Methodology, Conceptualization. **Ida B. Johansen:** Writing – review & editing, Resources, Funding acquisition. **Michael Frisk:** Writing – review & editing, Supervision, Resources, Project administration, Methodology, Investigation, Funding acquisition, Formal analysis, Data curation, Conceptualization.

Declaration of competing interest

The authors declare that they have no known competing financial interests or personal relationships that could have appeared to influence the work reported in this paper.

Data availability

Data will be made available on request.

Acknowledgements

The work was funded by the Norwegian Research Council (grant no. 303150), the Norwegian Seafood Research Fund (grant no. 901672), and University of Oslo.

References

Bartlett, J., Frost, C., 2008. Reliability, repeatability and reproducibility: analysis of measurement errors in continuous variables. Ultrasound Obstet. Gynecol.: Off. J. Intern. Soc. Ultrasound Obstet. Gynecol. 31, 466–475.
Berthoud, D., Schwarzwald, C.C., 2021. Echocardiographic assessment of left ventricular size and systolic function in warmblood horses using linear measurements, area-based indices, and volume estimates: a retrospective database analysis. J. Vet. Intern. Med. 35, 504–520.
Bland, J.M., Altman, D.G., 1996. Measurement error proportional to the mean. Br. Med. J. 313, 106.
Braun, M.H., Brill, R.W., Gosline, J.M., Jones, D.R., 2003. Form and function of the bulbus arteriosus in yellowfin tuna (*Thunnus albacares*): dynamic properties. J. Exp. Biol. 206, 3327–3335.
Brijs, J., Hjelmstedt, P., Berg, C., Johansen, I.B., Sundh, H., Roques, J.A.C., Ekström, A., Sandblom, E., Sundell, K., Olsson, C., Axelsson, M., Gräns, A., 2020. Prevalence and severity of cardiac abnormalities and arteriosclerosis in farmed rainbow trout (*Oncorhynchus mykiss*). Aquaculture 526, 735417.
Bunting, K.V., Steeds, R.P., Slater, L.T., Rogers, J.K., Gkoutos, G.V., Kotecha, D., 2019. A practical guide to assess the reproducibility of echocardiographic measurements. J. Am. Soc. Echocardiogr. 32, 1505–1515.
Casselman, M.T., Anttila, K., Farrell, A.P., 2012. Using maximum heart rate as a rapid screening tool to determine optimum temperature for aerobic scope in Pacific salmon Oncorhynchus spp. J. Fish Biol. 80, 358–377.
Chin Lai, N., Shabetai, R., Graham, J.B., Hoit, B.D., Sunnerhagen, K.S., Bhargava, V., 1990. Cardiac function of the leopard shark, Triakis semifasciata. J. Comp. Physiol. B 160, 259–268.
Cotter, P.A., Han, A.J., Everson, J.J., Rodnick, K.J., 2008. Cardiac hemodynamics of the rainbow trout (*Oncorhynchus mykiss*) using simultaneous Doppler echocardiography and electrocardiography. J. Exp. Zool. A Ecol. Genet. Physiol. 309, 243–254.
Coucelo, J., Joaquim, N., Coucelo, J., 2000. Calculation of volumes and systolic indices of heart ventricle from *Halobatrachus didactylus*: echocardiographic noninvasive method. J. Exp. Zool. 286, 585–595.
Dalton, N., Shabetai, R., Bhargava, V., Lai, N.C., Graham, J.B., 1998. Echocardiographic and hemodynamic determinations of the ventricular filling pattern in some teleost fishes. Physiol. Zool. 71, 157–167.
DeCara, J.M., Lang, R.M., Koch, R., Bala, R., Penzotti, J., Spencer, K.T., 2003. The use of small personal ultrasound devices by internists without formal training in echocardiography. Eur. J. Echocardiogr. 4, 141–147.
Decloedt, A., De Clercq, D., Ven Sofie, S., Van Der Vekens, N., Sys, S., Broux, B., van Loon, G., 2017. Echocardiographic measurements of right heart size and function in healthy horses. Equine Vet. J. 49, 58–64.
Demers, N.E., Bayne, C.J., 1997. The immediate effects of stress on hormones and plasma lysozyme in rainbow trout. Dev. Comp. Immunol. 21, 363–373.
Dukes-McEwan, J., French, A.T., Corcoran, B.M., 2002. Doppler echocardiography in the dog: measurement variability and reproducibility. Vet. Radiol. Ultrasound 43, 144–152.

Ellenberger, K., Jeyaprakash, P., Sivapathan, S., Sangha, S., Kitley, J., Darshni, A., Chen, D., Negishi, K., Pathan, F., 2022. The effect of obesity on echocardiographic image quality. Heart, Lung Circul. 31, 207–215.
Engdal, V.A., Dalum, A.S., Kryvi, H., Frisk, M., Torsvik, H., Hodne, K., Romstad, H., Johansen, I.B., 2024. State of the heart: anatomical annotation and assessment of morphological cardiac variation in Atlantic salmon (*Salmo salar* L.). Aquaculture 578, 740046.
Farrell, A.P., Smith, F., 2017. Cardiac form, function and physiology. In: Gamperl, A.K., Gillis, T.E., Farrell, A.P., Brauner, C.J. (Eds.), Fish Physiology. Elsevier, pp. 155–264.
Gentile-Solomon, J.M., Abbott, J.A., 2016. Conventional echocardiographic assessment of the canine right heart: reference intervals and repeatability. J. Vet. Cardiol. 18, 234–247.
Hill, J.V., Davison, W., Forster, M.E., 2002. The effects of fish anaesthetics (MS222, metomidate and AQUI-S) on heart ventricle, the cardiac vagus and branchial vessels from Chinook salmon (*Oncorhynchus tshawytscha*). Fish Physiol. Biochem. 27, 19–28.
Hsue, W., Visser, L.C., 2020. Reproducibility of echocardiographic indices of left atrial size in dogs with subclinical myxomatous mitral valve disease. J. Vet. Intern. Med. 34, 1779–1786.
Jiang, J., Strother, C., Johnson, K., Baker, S., Consigny, D., Wieben, O., Zagzebski, J., 2011. Comparison of blood velocity measurements between ultrasound Doppler and accelerated phase-contrast MR angiography in small arteries with disturbed flow. Phys. Med. Biol. 56, 1755–1773.
Kebed, K., Sun, D., Addetia, K., Mor-Avi, V., Markuzon, N., Lang, R.M., 2020. Measurement errors in serial echocardiographic assessments of aortic valve stenosis severity. Int. J. Card. Imaging 36, 471–479.
Labbé, V., Ederhy, S., Pasquet, B., Miguel-Montanes, R., Rafat, C., Hajage, D., Gaudry, S., Dreyfuss, D., Cohen, A., Fartoukh, M., Ricard, J.D., 2016. Can we improve transthoracic echocardiography training in non-cardiologist residents? Experience of two training programs in the intensive care unit. Ann. Intensive Care 6, 44.
Letnes, J.M., Eriksen-Volnes, T., Nes, B., Wisløff, U., Salvesen, Ø., Dalen, H., 2021. Variability of echocardiographic measures of left ventricular diastolic function. The HUNT study. Echocardiography 38, 901–908.
Linton, E., Scruton, D., McKinley, R.S., 2004. Cardiac output in fish: measurement techniques and applications. Can. Tech. Rep. Fish. Aquat. Sci. 2555 iv + 28p.
Ma, K.G., Gamperl, A.K., Syme, D.A., Weber, L.P., Rodnick, K.J., 2019. Echocardiography and electrocardiography reveal differences in cardiac hemodynamics, electrical characteristics, and thermal sensitivity between northern pike, rainbow trout, and white sturgeon. J. Exper. Zool. Part A: Ecol. Integr. Physiol. 331, 427–442.
McArley, T.J., Morgenroth, D., Zena, L.A., Ekström, A.T., Sandblom, E., 2021. Normoxic limitation of maximal oxygen consumption rate, aerobic scope and cardiac performance in exhaustively exercised rainbow trout (*Oncorhynchus mykiss*). J. Exp. Biol. 224.
Metcalfe, J.D., Butler, P.J., 1982. Differences between directly measured and calculated values for cardiac output in the dogfish: a criticism of the Fick method. J. Exp. Biol. 99, 255–268.
Mirea, O., Berceanu, M., Donoiu, I., Militaru, C., Săftoiu, A., Istrătoaie, O., 2019. Variability of right ventricular global and segmental longitudinal strain measurements. Echocardiography 36, 102–109.
Morgenroth, D., McArley, T., Gräns, A., Axelsson, M., Sandblom, E., Ekström, A., 2021. Coronary blood flow influences tolerance to environmental extremes in fish. J. Exp. Biol. 224.
Nekvasil, N.P., Olson, K.R., 1986. Plasma clearance, metabolism, and tissue accumulation of 3H-labeled catecholamines in trout. Am. J. Phys. Regul. Integr. Comp. Phys. 250, R519–R525.
Papolos, A., Narula, J., Bavishi, C., Chaudhry, F.A., Sengupta, P.P., 2016. US hospital use of echocardiography: insights from the nationwide inpatient sample. J. Am. Coll. Cardiol. 67, 502–511.
Quiñones, M.A., Otto, C.M., Stoddard, M., Waggoner, A., Zoghbi, W.A., 2002. Recommendations for quantification of Doppler echocardiography: a report from the Doppler quantification task force of the nomenclature and standards Committee of the American Society of echocardiography. J. Am. Soc. Echocardiogr. 15, 167–184.
Randall, D.J., Ferry, S.F., 1992. Catecholamines. In: Hoar, W.S., Randall, D.J., Farrel, A. P. (Eds.), Fish Physiology. Academic Press, pp. 255–300.
Randall, D.J., Smith, L.S., 1967. The effect of environmental factors on circulation and respiration in teleost fish. Hydrobiologia 29, 113–124.
Reef, V.B., 1991. Advances in echocardiography. Vet. Clin. N. Am. Equine Pract. 7, 435–450.
Ryan, S.N., Davie, P.S., Gesser, H., Wells, R.M.G., 1993. The effect of MS-222 on paced ventricle strips and the perfused heart of rainbow trout, *Oncorhyncus mykiss*. Comp. Biochem. Physiol. C: Pharmacol. Toxicol. Endocrinol. 106, 549–553.
Sandblom, E., Axelsson, M., Davison, W., 2009. Circulatory function at sub-zero temperature: venous responses to catecholamines and angiotensin II in the Antarctic fish *Pagothenia borchgrevinki*. J. Comp. Physiol. B. 179, 165–173.
Sande, R.D., Poppe, T.T., 1995. Diagnostic ultrasound examination and echocardiography in Atlantic salmon (*Salmo salar*). Veterin. Radiol. Ultrasound 36 (6), 551–558.
Sandrelli, R.M., Gamperl, A.K., 2023. The upper temperature and hypoxia limits of Atlantic salmon (*Salmo salar*) depend greatly on the method utilized. J. Exp. Biol. 226.
Schindelin, J., Arganda-Carreras, I., Frise, E., Kaynig, V., Longair, M., Pietzsch, T., Preibisch, S., Rueden, C., Saalfeld, S., Schmid, B., Tinevez, J.-Y., White, D.J., Hartenstein, V., Eliceiri, K., Tomancak, P., Cardona, A., 2012. Fiji: an open-source platform for biological-image analysis. Nat. Methods 9, 676–682.
Sjaastad, I., Sejersted, O.M., Ilebekk, A., Bjørnerheim, R., 2000. Echocardiographic criteria for detection of postinfarction congestive heart failure in rats. J. Appl. Physiol. 89, 1445–1454.
Skals, M., Skovgaard, N., Taylor, E.W., Leite, C.A.C., Abe, A.S., Wang, T., 2006. Cardiovascular changes under normoxic and hypoxic conditions in the air-breathing teleost *Synbranchus marmoratus*: importance of the venous system. J. Exp. Biol. 209, 4167–4173.
Sommerset, I., Wiik-Nielsen, J., Oliveira, V.H.S., Moldal, T., Bornø, G., Haukaas, A., Brun, E., 2023. Norwegian Fish Health Report 2022, Norwegian Veterinary Institute Report, series #5a/2023, published by the Norwegian Veterinary Institute in 2023.
Tanaka, N., Dalton, N., Mao, L., Rockman, H.A., Peterson, K.L., Gottshall, K.R., Hunter, J. J., Chien, K.R., Ross, J., 1996. Transthoracic echocardiography in models of cardiac disease in the mouse. Circulation 94, 1109–1117.
Tournoux, F., Petersen, B., Thibault, H., Zou, L., Raher, M.J., Kurtz, B., Halpern, E.F., Chaput, M., Chao, W., Picard, M.H., Scherrer-Crosbie, M., 2011. Validation of noninvasive measurements of cardiac output in mice using echocardiography. J. Am. Soc. Echocardiogr. 24, 465–470.
Usui, Y., Kimoto, M., Hanashima, A., Hashimoto, K., Mohri, S., 2022. Cardiac hemodynamics and ventricular stiffness of sea-run cherry salmon (*Oncorhynchus masou masou*) differ critically from those of landlocked masu salmon. PLoS One 17, e0267264.
Vignon, P., Mücke, F., Bellec, F., Marin, B., Croce, J., Brouqui, T., Palobart, C., Senges, P., Truffy, C., Wachmann, A., Dugard, A., Amiel, J.B., 2011. Basic critical care echocardiography: Validation of a curriculum dedicated to noncardiologist residents. Crit. Care Med. 39, 636–642.
Wang, L.W., Huttner, I.G., Santiago, C.F., Kesteven, S.H., Yu, Z.-Y., Feneley, M.P., Fatkin, D., 2017. Standardised echocardiographic assessment of cardiac function in normal adult zebrafish and heart disease models. Dis. Model. Mech. 10, 63–76.
Winkler, A.J., Wu, J., 1995. Correction of intrinsic spectral broadening errors in Doppler peak velocity measurements made with phased sector and linear array transducers. Ultrasound Med. Biol. 21, 1029–1035.
Zena, L.A., Ekström, A., Morgenroth, D., McArley, T., Gräns, A., Axelsson, M., Johansen, I.B., Sandblom, E., 2024. Ischemia-induced alterations in the electrocardiogram of salmonid fish. Aquaculture 581 (740), 482.